ANALYSIS OF GRAPH-BASED USER SCHEDULING FOR KA-BAND LEO NTN SYSTEMS

Bilal Ahmad[1], Daniel Gaetano Riviello[1], Bruno De Filippo[1], Alessandro Guidotti[2], Alessandro Vanelli-Coralli[1]
[1]Department of Electrical, Electronic, and Information Engineering (DEI), Univ. of Bologna, Bologna, Italy,
[2]National Inter-University Consortium for Telecommunications (CNIT), Univ. of Bologna Research Unit, Italy,
Emails: bilal.ahmad6@unibo.it, daniel.riviello@unibo.it, bruno.defilippo2@unibo.it, a.guidotti@unibo.it, alessandro.vanelli@unibo.it,

Abstract

This work focuses on the next generations of multi-beam (MB) Low Earth Orbit (LEO) based Non-Terrestrial Network (NTN) architectures that exploit full spectrum reuse schemes and effective interference management techniques by employing user scheduling before precoding at the transmit side. Given a high density of user terminals (UTs) on-ground as compared to on-board LEO satellite antennas it is extremely challenging to schedule users. To improve the performance, optimal user scheduling is necessary. In this paper, we present the analysis of graph-based user scheduling algorithms for Ka-band, with a focus on feed space (FS), downlink (DL), and Frequency Division Duplex (FDD) mode. We propose both a distance-based iterative graph-based approach and a distance-based implementation of the Multiple Antenna Downlink Orthogonal User Clustering (MADOC) algorithm. Instead of considering the Coefficient of Correlation (CoC) as a dissimilarity measure to organize users into clusters, we consider the great circle distance between the users as a dissimilarity metric. Once users are organized into clusters, they are served by the LEO satellite using Space Division Multiplexing (SDM) through Minimum Mean Square Error (MMSE) beamforming applied per cluster. Subsequently, these clusters are allocated to different time slots using Time Division Multiplexing (TDM). To validate the effectiveness of our presented approach, we conduct a comparative analysis with the original Channel State Information (CSI)-based MADOC algorithm which is based on the CoC. The results are presented in terms of the achievable per-user throughput (Mbps), and signal-to-noise plus interference ratio (SINR). By considering user scheduling and beamforming together, this study provides valuable insights into the effective use of resources in LEO MB-NTN systems.

1. Introduction

NTN systems are expected to play a significant role in future generations of wireless networks. The primary motivator is that, due to their intrinsic characteristics, these systems can integrate and complement terrestrial coverage, extending the provision of data access to all geographical locations, where the terrestrial coverage is not available or financially viable [1]. With the approval of 3GPP Rel-17 and the inclusion of NTN systems in 5G-Advanced and 6G systems, the satellite industry is undergoing rapid growth, paving the way for global access to 6G services [2]. LEO-based NTN when compared with the Geostationary Earth Orbit (GEO) satellites possess the advantage of lower propagation delay, reduced path loss, and less stringent power requirements. Thanks to lower latency, LEO technology can be utilized for real-time and time-sensitivity applications. However, the main challenge for future generations of wireless networks will be to meet the growing demand for new services while dealing with the scarcity of the frequency spectrum.

Legacy Satellite Communication (SATCOM) systems use multi-color frequency reuse schemes to spatially reuse the available resources while minimizing interference from beam-side lobes. To improve the spectral efficiency, Full Frequency Reuse (FFR) schemes can be employed in LEO NTN systems, where all the beams use the same frequency band with a single color. In literature, linear precoding techniques are widely studied to mitigate the Co-Channel Interference (CCI). However, the performance of precoding heavily relies on the geographical distribution of UTs; if the users are too close to each other, the performance of the precoding may substantially decrease [3, 4].

LEO satellites with an onboard antenna array can offer service to numerous on-ground UTs (VSAT or Handhelds) in FFR schemes employing digital beamforming techniques in the FS. But, when the number of UTs becomes extremely high, the interference will significantly reduce the LEO's throughput. To tackle this issue, user scheduling can be accomplished by grouping users into clusters: users within the same group are simultaneously served by the satellite via SDM and the different clusters are served in different time slots via TDM [4, 5]. The challenge for every user scheduling algorithm is to find the optimal subset of UTs. Given this optimization problem is NP-complete, the current trend is to design suboptimal solutions to balance complexity and performance. An interesting solution is the CSI-based "Multiple Antenna Downlink Orthogonal User Clustering" (MADOC) algorithm which is based on the coefficient of correlation matrix [6], which will have considered as a benchmark solution for this work.

In the paper, we extend our work in [7-9] and provide a thorough description of a novel Radio Resource Management (RRM) algorithm, i.e., a graph-based scheduling algorithm that allows to proper selection of a subset of users for each time slot and serve them by employing feed space precoding techniques for the Ka-band. Our previous work [7-9] considered the S-band. Moreover, now we propose a new grouping indicator for both the graph-based scheduler and MADOC, which only relies on the users' locations and does not require the knowledge of Channel State Information (CSI) at the scheduling phase. The primary objective is to maximize the sum-rate capacity of the system while ensuring fairness among its users.

To tackle this challenge, we first formulate the user clustering problem as an undirected and unweighted graph. In this graph, each vertex corresponds to a UT, and the edges are determined between two users and are established if their great-circle distance exceeds a certain threshold. By adopting this method, we solely rely on the knowledge of user positions and not the CSI at the transmitter during the scheduling phase. Once the graph is constructed, our scheduling procedure iteratively seeks the maximum clique, representing the largest fully connected subgraph, using the efficient maximum clique dyn algorithm approach [10]. The vertices within this clique are then assigned to a cluster, removed from the graph, and the process is reiterated until no users remain to be scheduled. Within each cluster, SDM is achieved through FS MMSE beamforming. Furthermore, we explore two distinct power normalization schemes for the beamforming matrix: Sum Power Constraint (SPC) and Maximum Power Constraint (MPC) [11]. To optimize the system's performance, we employ a heuristic approach to find the optimized threshold value that maximizes the per-user throughput (Mbps).

2. System Model

To keep consistency in the work, the presented system model has been adopted from our previously presented work [7-9]. A standalone LEO satellite equipped with an onboard planar antenna array is considered here. The antenna array consists of N radiating elements which provide connectivity to a total of K single-antenna uniformly distributed on-ground users utilizing $S \leq N$ beams. Our further assumptions are based on the system architecture comprehensively explained in [7-9]. The on-ground gNB is responsible for the user grouping, i.e., RRM and computation of the beamforming coefficients. Both scheduling and beamforming require the estimation of CSI which is provided by the UTs. The CSI values are computed by the users at time instant t_0; The scheduling and the beamforming matrices for every group of users are then computed at the gNB and used to transmit the beamformed symbols to the users at time $t_0 + \Delta t$. The latency Δt between the channel estimation phase and the transmission phase introduces a misalignment between the channel on which the scheduling and the beamforming matrices are computed and the actual channel through which the transmission occurs, which impacts the system performance. The latency is due to

$$\Delta t = t_{ut,max} + 2t_{feeder} + t_p + t_{ad} \quad (1)$$

Where:

i. $t_{ut,max}$ is the maximum propagation delay for the UTs requesting connectivity in coverage.
ii. t_{feeder} is the propagation delay on the feeder link, considered twice since the estimates are to be sent to the GW on the return link and then the beamformed symbols are sent on the forward link to the satellite.
iii. t_p is the processing delay needed to compute the beamforming matrix, and
iv. t_{ad} includes any additional delay. The antenna array model assumed here is based on ITU-R Recommendation M.2101 as illustrated in the Fig. 1 [12].

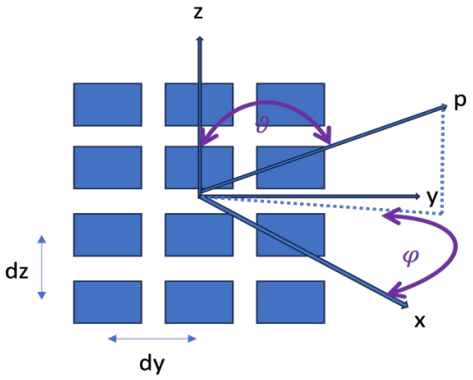

Fig. 1: MB Antenna Array Model from ITU-R M.2101-0 [12].

By default, the antenna boresight direction is defined by the direction of the Sub-Satellite Point (SSP). The point P is the position of the user terminal on the ground. The user directions are identified by (ϑ, φ) angles where the boresight direction is (0,0). We can now derive the direction cosines for the considered user as $u = \frac{P_y}{\|P\|}\sin\vartheta\sin\varphi$, and $v = \frac{P_z}{\|P\|}\cos\vartheta$. The total array response of the Uniform Planar Array (UPA) in the generic direction (ϑ_i, φ_i) can be expressed as the Kronecker product of the array responses of the 2 Uniform Linear Arrays (ULAs) lying on the y- and z-axis. We first define the $1 \times N_H$ steering vector (SV) of the ULA along the y-axis $\mathbf{a}_H(\theta_i, \varphi_i)$ and the $1 \times N_V$ SV of the ULA along the z-axis $\mathbf{a}_V(\theta_i)$:

$$\mathbf{a}_H(\vartheta_i, \varphi_i) = \left[1, e^{jk_0 d_H \sin\vartheta_i \sin\varphi_i}, \dots, e^{jk_0 d_H (N_H-1)\sin\vartheta_i \sin\varphi_i}\right] \quad (2)$$

$$\mathbf{a}_V(\vartheta_i) = \left[1, e^{jk_0 d_V \cos\vartheta_i}, \dots, e^{jk_0 d_V (N_V-1)\cos\vartheta_i}\right] \quad (3)$$

Where:

$k_0 = 2\pi\lambda$ is the wave number, N_H, N_V denotes the number of array elements on the horizontal (y-axis) and vertical (z-axis) directions with $N = N_H \cdot N_V$ and d_H, d_V denote the distance between adjacent array elements on the y-and z-axis respectively. We assume that the array is equipped with directive antenna elements, whose radiation pattern is denoted by $g_E(\vartheta_i, \varphi_i)$. Finally, we can express the $1 \times N$ SV of the UPA at the satellite targeted for the i-th user as the Kronecker product of the 2 SVs along each axis multiplied by the element radiation pattern:

$$\mathbf{a}(\vartheta_i, \varphi_i) = g_E(\vartheta_i, \varphi_i)\, \mathbf{a}_H(\vartheta_i, \varphi_i) \otimes \mathbf{a}_V(\vartheta_i) \quad (4)$$

The CSI vector at feed level $\hat{\mathbf{h}}_i$ represents the channel between the N radiating elements and the generic i-th on-ground UT, with $i = 1, \dots, K$, can be written as:

$$\hat{\mathbf{h}}_i = G_i^{(rx)} \frac{\lambda}{4\pi d_i} \sqrt{\frac{L_i}{\kappa B T_i}}\, e^{-j\frac{2\pi}{\lambda} d_i} \mathbf{a}(\vartheta_i, \varphi_i) \quad (5)$$

in which, d_i is the slant range between the generic i-th user and the satellite, λ is the wavelength, $\kappa B T_i$ denotes the equivalent thermal noise power, with κ being the Boltzmann constant, B the user bandwidth (assumed to be the same for all users), and T_i the equivalent noise temperature of the i-th UT. $G_i^{(rx)}$ denotes the receiving antenna gain for the i-th UT, while L_i denotes all the additional losses per user, such as for example atmospheric, antenna, and cable losses. More in detail, the additional losses are computed based on 3GPP TR 38.821 as:

$$L_i = L_{sha,i} + L_{atm,i} + L_{sci,i} \quad (6)$$

where $L_{sha,i}$ represents the log-normal shadow fading term, $L_{atm,i}$ the atmospheric loss, and $L_{sci,i}$ the scintillation. Collecting all of the K CSI vectors, it is possible to build a $K \times N$ complex channel matrix at system level $\hat{\mathbf{H}} = \left[\hat{\mathbf{h}}_1^{\mathrm{T}}, \hat{\mathbf{h}}_2^{\mathrm{T}}, \dots, \hat{\mathbf{h}}_K^{\mathrm{T}}\right]^{\mathrm{T}}$, where the generic k-th row contains the CSI vector of the k-th user and the generic n-th column contains the channel coefficients from the n-th on-board feed towards the K on-ground users.

Given the set of all users to be scheduled, denoted with $\mathcal{U} = \{U_1, U_2, \dots, U_K\}$, the RRM algorithm defines a possible users' partitioning $\{\mathcal{C}_1, \mathcal{C}_2, \dots, \mathcal{C}_P\}$ where $\mathcal{C}_p \subseteq \mathcal{U}$ is defined as cluster and $|\mathcal{C}_p| = K_p$ is defined as the cardinality of the p-th cluster with $p = 1, \dots, P$. Clusters are not necessarily disjoint sets of users, clearly $|\mathcal{C}_1 \cup \mathcal{C}_2 \cup \dots \cup \mathcal{C}_P| = K$. In each time slot, users belonging to cluster $\mathcal{C}_p$ are selected, leading to a $K_p \times N$ complex scheduled channel matrix $\hat{\mathbf{H}}_p \subseteq \hat{\mathbf{H}}$, which contains only the rows of the scheduled users in the p-th cluster. The selected beamforming algorithm computes for each cluster a $N \times K_p$ complex beamforming matrix $\mathbf{W}_p = \left[\mathbf{w}_1^{(p)}, \mathbf{w}_2^{(p)}, \dots, \mathbf{w}_{K_p}^{(p)}\right]$, where $\mathbf{w}_i^{(p)}$ denotes the $N \times 1$ beamformer designed for the i-th user in the p-th cluster. The matrix $\mathbf{W}_p$ projects the K_p dimensional column vector $\mathbf{s}_p = \left[s_1, s_2, \dots, s_{K_p}\right]^{\mathrm{T}}$ containing the unit-variance user symbols onto the N-dimensional space defined by the antenna feeds. Thus, in the feed space, the computation of the beamforming matrix allows for the generation of a dedicated beam towards each user direction. The signal received by the i-th user in the p-th cluster can be expressed as follows:

$$y_k^{(p)} = \mathbf{h}_k \mathbf{w}_k^{(p)} s_k + \sum_{\substack{i=1 \\ i \neq k}}^{K_p} \mathbf{h}_k \, \mathbf{w}_i^{(p)} s_i + z_k^{(p)} \tag{7}$$

where $z_k^{(p)}$ is a circularly symmetric Gaussian random variable with zero mean and unit variance. The K_p-dimensional vector of received symbols in the p-th cluster is:

$$\mathbf{y}_p = \mathbf{H}_p \mathbf{W}_p \mathbf{s}_p + \mathbf{z}_p \tag{8}$$

It shall be noted that, as previously discussed, the estimated channel matrix $\hat{\mathbf{H}}$ at time t_0 is used to compute the scheduling and the beamforming matrices $\mathbf{W}_p$ in the estimation phase, while the beamformed symbols are sent to the users at a time instant $t_0 + \Delta t$, in which the scheduled channel matrices and vectors are different and denoted as $\mathbf{H}_p$ and $\mathbf{h}_k$, respectively.

The SINR for user k belonging to cluster p can be computed as:

$$\mathrm{SINR}_k^{(p)} = \frac{\left\|\mathbf{h}_k \mathbf{w}_k^{(p)}\right\|^2}{1 + \sum_{\substack{i=1 \\ i \neq k}}^{K_p} \left\|\mathbf{h}_k \mathbf{w}_i^{(p)}\right\|^2} \tag{9}$$

Given a TDM time frame T_F, each cluster is assigned a time slot T_p. To design a fair-proportional scheduler, we assume that we can adjust the duration of each time slot T_p to be proportional to the cardinality of each cluster K_p, i.e.,

$$T_p = \gamma_p \, T_F \tag{10}$$

$$\gamma_p = \frac{K_p}{\sum_{p=1}^{P} K_p} \tag{11}$$

Therefore, to consider, the duty cycle associated with each cluster, we can define the user throughput as:

$$C_k = B \sum_{\substack{p \\ U_k \in \mathcal{C}_p}} \gamma_p \log_2\left(1 + \mathrm{SINR}_k^{(p)}\right) \tag{12}$$

where γ_p denotes the cluster weight. The beamforming matrix $\mathbf{W}_p$, which is computed on a cluster basis, is based on the linear MMSE equation:

$$\mathbf{W}_p = \hat{\mathbf{H}}_p^H (\hat{\mathbf{H}}_p \hat{\mathbf{H}}_p^H + \alpha \mathbf{I}_{K_p})^{-1} \tag{13}$$

where $\mathbf{I}_{K_p}$ indicates the $K_p \times K_p$ identity matrix and $\alpha = \frac{N}{P_t}$ is the regularisation factor with P_t the total on-board power. Finally, as detailed in [11], the power normalization is a fundamental step for beamforming to properly consider the power that can be emitted both by the satellite and per antenna. We consider the following two options for power normalization i.e., SPC and MPC and defined as:

$$\text{SPC} \rightarrow \widetilde{\mathbf{W}}_p = \frac{\sqrt{P_t}\mathbf{W}_p}{\sqrt{\text{tr}\left(\mathbf{W}_p \mathbf{W}_p^H\right)}} \tag{14}$$

$$\text{MPC} \rightarrow \widetilde{\mathbf{W}}_p = \frac{\sqrt{P_t}\mathbf{W}_p}{\sqrt{N \max_j \left[\mathbf{W}_p \mathbf{W}_p^H\right]_{j,j}}} \tag{15}$$

3. User Scheduling

In this section we provide the description of the distance-based Maximum Clique Scheduler [8] and we present the novel distance-based implementation of the MADOC algorithm.

A. Distance-based Maximum Clique Scheduler

We denote with $\mathcal{G} = (\mathcal{V}, \mathcal{E})$ an undirected and unweighted graph with vertex set $\mathcal{V}$ and edge set $\mathcal{E}$. A clique $\mathcal{Q}$ of $\mathcal{G}$ is a subset of the vertices, $\mathcal{Q} \subseteq \mathcal{V}$, such that every two distinct vertices are adjacent, i.e., $\mathcal{Q}$ is a complete subgraph. In our considered scenario, the set of vertices $\mathcal{V}$ coincides with the set of users $\mathcal{U}$ and the edge set is constructed based on a dissimilarity measure, which is the users' great circle distance. Given the latitudes, ϕ_i and ϕ_j of the users i and j, respectively, and λ_i and λ_j their respective longitudes, their great circle distance can be computed through the haversine formula.
We first define:

$$h = \sin^2\left(\frac{\phi_j - \phi_i}{2}\right) + \cos\phi_i \cdot \cos\phi_j \cdot \sin^2\left(\frac{\lambda_j - \lambda_i}{2}\right) \tag{16}$$

then:

$$[\mathbf{\Gamma}]_{i,j} = 2r\text{arcsin}\left(\sqrt{h}\right) \tag{17}$$

After that we can now define the corresponding adjacency matrix $\mathbf{A}$ as:

$$[\mathbf{A}]_{i,j} = \begin{cases} 1, & [\mathbf{\Gamma}]_{i,j} \geq \delta_D \\ 0, & [\mathbf{\Gamma}]_{i,j} < \delta_D \end{cases} \tag{18}$$

where δ_D is again a properly designed threshold. If an element of $\mathbf{A}$ is equal to 1, the great-circle distance and therefore the angular distance between U_i and U_j is such that their directions (ϑ_i, φ_i) and (ϑ_j, φ_j) can be spatially separated by means of MMSE digital beamforming, and they can belong to the same cluster (or they can be co-scheduled), while if an element of $\mathbf{A}$ is equal to 0, the directions of U_i and U_j are considered to be too close to be spatially distinguished by the beamformer.

The threshold determines an upper bound on the size of a clique and therefore the optimal number of users that can be efficiently multiplexed in the space domain by MMSE beamforming within a cluster. A maximum clique $\mathcal{Q}_{\max} \subseteq \mathcal{V}$ is a clique, such that there is no clique with more vertices. The proposed user scheduling algorithm is a greedy iterative procedure that aims at minimizing the total number of clusters P, given an optimized threshold δ_D for the distance-based case and accomplished by:

1. maximizing the size of each cluster by iteratively finding the maximum clique of the updated graph.
2. creating disjoint sets of scheduled users, i.e., $\mathcal{C}_i \cap \mathcal{C}_j = \varnothing,\ \forall i,j$, which also minimizes the total number of clusters P.

The maximum clique problem has been widely investigated in the current state-of-the-art (SOA). Several algorithms have been proposed for the exact solution of the problem, but also various efficient heuristic algorithms have been developed, which allow to solve the problem in polynomial time. In this work, we implemented and Improved the Maximum Clique DYN (MCD) algorithm to find the best optimal largest maximum clique. A comprehensive analysis on different algorithms can be found in [10]. We presented the algorithm in [ref], which illustrates that the iterative procedure searches for the maximum clique $\mathcal{Q}_{\max}$ in the graph and declares it as a cluster; at each step, the nodes in $\mathcal{Q}_{\max}$ and any edges connected to them are removed, the graph is updated after pruning. The procedure is repeated until there are no more vertices in the graph. Fairness is guaranteed among users by setting the cluster weight $\gamma_p = \frac{K_p}{K}$, which defines the duration of the time slot T_p assigned to cluster $\mathcal{C}_p$ within the total TDM time frame T_F

B. Distance-based MADOC

The original CSI-based MADOC algorithm [6] evaluates the spatial computability of two users that can be co-scheduled and served together within a common time slot via SDM by considering the coefficient of correlation matrix provided in equation (19). Fairness is ensured by trying to provide similar data rates to every group and every user within a group.

$$\mathrm{CoC}(U_i, U_j) = \frac{\left|\widehat{\boldsymbol{h}}_i \widehat{\boldsymbol{h}}_j^H\right|}{\|\widehat{\boldsymbol{h}}_i\| \|\widehat{\boldsymbol{h}}_j\|} \tag{19}$$

Instead of evaluating the spatial compatibility of two users based on coefficient of correlation matrix, differently in this work, as presented in Algorithm 1, we propose a distance-based MADOC algorithm that considers the users' inter-distance matrix as a grouping indicator based on (16) and (17).

The distance-based MADOC algorithm only requires the users' positions in order to compute their slant ranges d_i and their inter-distances $[\boldsymbol{\Gamma}]_{i,j}$. As illustrated in Algorithm 1, the procedure first identifies the minimum number of required clusters. In the original MADOC, the P users with the largest channel vector norm are selected to be the first user of each cluster, instead we select the P users with the shortest slant range. In the main part of the algorithm, for every selected user v, the cluster $\mathcal{C}_s$ is selected such that the inter-distances between v and all other users belonging to cluster $\mathcal{C}_s$ are as high as possible: if all inter-distances in $\mathcal{C}_s \cup \{v\}$ are above a certain threshold ϵ_D, user v is added into cluster $\mathcal{C}_s$, otherwise a new cluster is created. Finally, v is removed from the user set $\mathcal{U}$ and the procedure is repeated until there are no more users to be scheduled.

Algorithm 1: Distance-based MADOC Algorithm

Procedure CLUSTER_USERS ($\mathcal{U}, N, \boldsymbol{d}$)
$\mathcal{U} = \{U_1, U_2, \dots, U_K\}$ is the set of all users to be scheduled, $K = |\mathcal{U}|$
N is the total no. of feeds (32x32)
$\boldsymbol{d} = [d_1, d_2, \dots, d_K]$ is the vector of users' slant ranges
$P = [K/N]$
$\mathcal{C}_1 = \dots = \mathcal{C}_P = \emptyset$
for $p \leftarrow 1$ **to** P **do**
$v = \underset{U_k \in \mathcal{U}}{\arg\min}\, d_k$

$\mathcal{C}_p = \{v\}$
$\mathcal{U} = \mathcal{U} \setminus \{v\}$
end for
while $|\mathcal{U}| > 0$ **do**
$v = \arg\min_{U_k \in \mathcal{U}} d_k$
$s = \arg\max_{1 \le p \le P} \left(\min_{U_i \in \mathcal{C}_p} [\mathbf{\Gamma}]_{v,i} \right)$ $[\mathbf{\Gamma}]_{v,i}$ is computed as in (16) and (17)
if $\left(\min_{U_i \in \mathcal{C}_p} [\mathbf{\Gamma}]_{v,i} > \epsilon_D \right)$ **then**
$\mathcal{C}_s = \mathcal{C}_s \cup \{v\}$
else
$P = P + 1$
$\mathcal{C}_P = \{u\}$
end if
$\mathcal{U} = \mathcal{U} \setminus \{v\}$
end while
end procedure

4. Simulation Results

In this section, we present the results of extensive numerical simulations using the parameters specified in Tab. 1. These assessments were conducted under optimal buffer conditions. We focused our analysis on standalone LEO satellite positioned at 600 kilometers from Earth. On average, the total number of users in this scenario amounts to $K = 2850$. The LEO satellite is equipped with a UPA of 32x32 feeds. UTs remain stationary, and their receiver antenna gain $G_{\max}^{(rx)}$ is set to 39.7 dBi. The adopted propagation model is the Line of Sight, based on 3GPP TR 38.811 and TR 38.821 [13-14].

Tab. 1: Simulation Parameters

Carrier frequency	20 GHz	Propagation scenario	Line of Sight
System Band	Ka	System scenario	Urban
Beamforming space	Feed	Total on-board power density $P_{t,\text{dens}}$	4 dBW/MHz
Receiver type	VSAT	User density	0.05 users/km^2
Receiver antenna gain	39.7 dBi	Number of transmitters	1024 (32 x 32 UPA)
Noise Figure	1.2 dB	Receiver scenario	Fixed

Aiming at maximizing the average user throughput, we performed a heuristic optimization of thresholds ϵ_C for original MADOC scheduler (CSI-based), ϵ_D for the newly proposed distance-based MADOC scheduler, and δ_D for the distance-based maximum clique scheduler.

Fig. 2 illustrates that the optimized thresholds ϵ_C for original MADOC scheduler (CSI-based) is 0.48 for MMSE-SPC and 0.38 for MMSE-MPC.

Fig. 3 illustrates that the optimized thresholds ϵ_D for the newly proposed distance-based MADOC scheduler is 26 km for MMSE-SPC and 28 km for MMSE-MPC.

Fig. 4 illustrates that the optimized thresholds δ_D for the distance-based maximum clique scheduler is 29.5 km for MMSE-SPC and 31 km for MMSE-MPC.

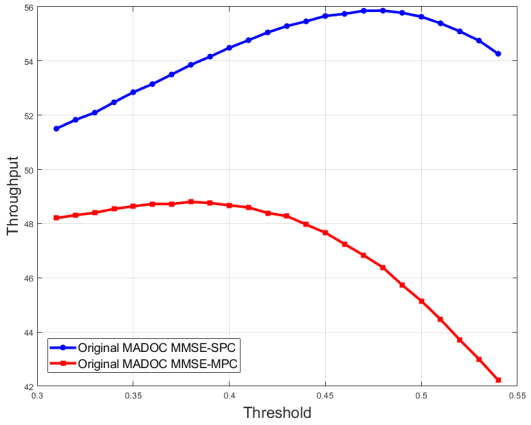

Fig. 2: Threshold optimization for original MADOC (CSI-based).

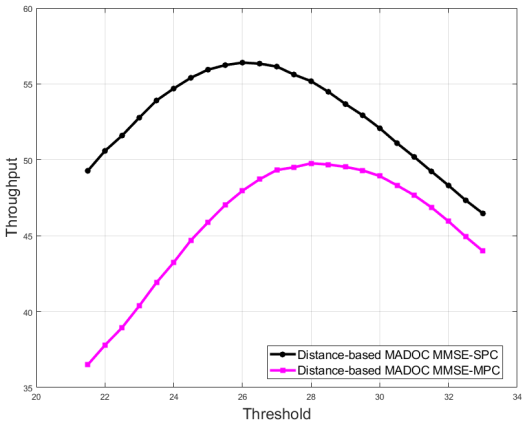

Fig. 3: Threshold Optimization for distance-based MADOC.

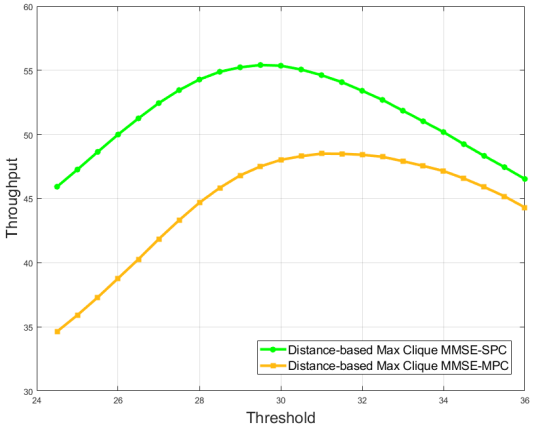

Fig. 4: Threshold Optimization for distance-based Maximum Clique scheduler.

Tab. 2 provides a comprehensive summary of the results for each scheduler. It includes the optimal threshold values, the mean cluster size, throughput in Mbps, and SINR in dB. The user throughput calculations were performed using a per-cluster MMSE beamforming matrix, incorporating SPC and MPC power normalizations. Fig. 5 illustrates the Cumulative Distribution Function (CDF) of the users' throughput, while Fig. 6 illustrates the CDF of the users' SINR.

It can be noticed that the distance-based MADOC is able to slightly outperform the original CSI-based MADOC, while the distance-based maximum clique scheduler shows a performance very close to both MADOC approaches with a reduced mean cluster size. Additionally, in general, SPC normalization tends to accommodate larger user groups compared to MPC. From Fig. 5, we can also deduce that the both MADOC approaches show a slight better fairness among users w.r.t. to the distance-based maximum clique scheduler. From Fig. 6, the distribution of the users' SINR shows an almost identical pattern for MMSE-SPC while some differences are more evident for MMSE-MPC. ,. However, it's important to note that this does not completely discard the CSI knowledge as this is required during the transmission phase on a cluster level.

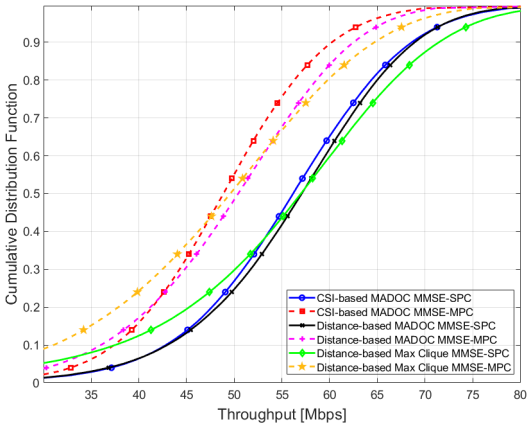

Fig. 5: CDF of users' throughput.

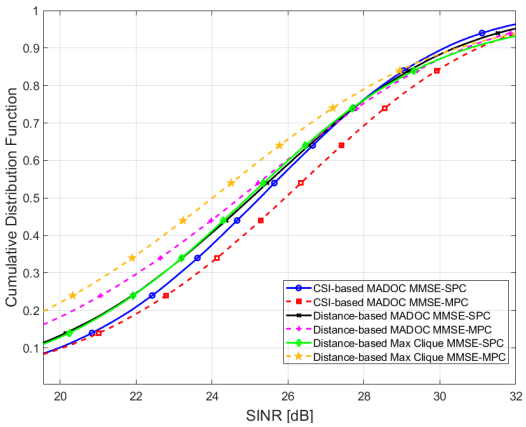

Fig. 6: CDF of users' SINR.

Tab. 2: Simulation Results for Schedulers with Threshold Optimizations				
Parameters	**Normalization**	**Original MADOC (CSI-based)**	**Distance-based MADOC**	**Distance-based Maximum Clique Scheduler**
Thresholds ϵ_C, ϵ_D, and δ_D	MMSE-SPC	0.48	26	29.5
	MMSE-MPC	0.38	28	31
Mean Cluster Size	MMSE SPC	46.07	49.25	39.97
	MMSE-MPC	39.39	44.05	37.03
Throughput [Mbps]	MMSE-SPC	55.86	56.41	55.42
	MMSE-MPC	48.80	49.77	48.51
SINR [dB]	MMSE-SPC	25.12	24.89	25.06
	MMSE-MPC	25.70	24.49	23.96

5. Conclusion

In this paper, we have proposed two user scheduling procedures that use as grouping indicator the users' great circle distance: a distance-based maximum clique algorithm and a distance-based MADOC variation of the original CSI-based algorithm. Within each cluster, we employ a digital MMSE beamforming matrix to achieve spatial separation among the scheduled users. Notably, we explored two distinct power normalization techniques for the MMSE matrix: SPC and MPC. In our presented analysis, we thoroughly determined the optimal threshold values for both distance-based schedulers and for the original MADOC The outcomes of our study have been presented in terms of user throughput and SINR and have shown that the distance-based grouping indicator can be highly competitive in the design of user scheduling algorithms.

6. Acknowledgement

This work is supported by 6G-NTN project which has received funding from the Smart Networks and Services Joint Undertaking (SNS JU) under the European Union's Horizon Europe research and innovation programme under Grant Agreement No 101096479. This work has received funding from the Swiss State Secretariat for Education, Research, and Innovation (SERI). The project aims to design and validate NTN's key technical, regulatory, and standardization enablers for the integration of TN and NTN components into 6G, focusing on multidimensional network infrastructure, multi-constraint RANs, and multi-user terminals.

7. References

[1]. Di Mezza, A. Vanelli Coralli, A. Guidotti, T. Foggi, G. Colavolpe and G. Montorsi, “5G4SPACE: Adaptation of 5G radio access technology for Satcom.” 2019 International Symposium on Advanced Electrical and Communication Technologies (ISAECT), Rome, Italy, 2019, pp. 1-3, doi: 10.1109/ISAECT47714.2019.9069675.

[2]. Guidotti, et.al, “Eager White paper- Architectures, Services, and Technologies towards 6G-NTN Systems.” Available online: *https://www.eagerproject.eu/scientific-publications/2022/08/16/eager-white-paper/*

[3]. A. Ugolini, Y. Zanettini, A. Piemontese, A. Vanelli-Coralli and G. Colavolpe, “Efficient satellite systems based on interference management and exploitation.” 2016 50th Asilomar Conference on Signals, Systems and Computers, Pacific Grove, CA, USA, 2016, pp. 492-496, doi: 10.1109/ACSSC.2016.7869088.

[4]. Guidotti, Alessandro, and Alessandro Vanelli-Coralli. “Clustering strategies for multicast precoding in multibeam satellite systems.” International Journal of Satellite Communications and Networking 38.2 (2020): 85-104.

[5]. X. Yi and E. K. S. Au, “User Scheduling for Heterogeneous Multiuser MIMO Systems: A Subspace Viewpoint.” in IEEE Transactions on Vehicular Technology, vol. 60, no. 8, pp. 4004-4013, Oct. 2011, doi: 10.1109/TVT.2011.2165976.

[6]. K. -U. Storek and A. Knopp, “Fair User Grouping for Multibeam Satellites with MU-MIMO Precoding.” GLOBECOM 2017 - 2017 IEEE Global Communications Conference, Singapore, 2017, pp. 1-7, doi: 10.1109/GLOCOM.2017.8255098.

[7]. D. G. Riviello, B. Ahmad, A. Guidotti and A. Vanelli-Coralli, “Joint Graph-based User Scheduling and Beamforming in LEO-MIMO Satellite Communication Systems.” 2022 11th Advanced Satellite Multimedia Systems Conference and the 17th Signal Processing for Space Communications Workshop (ASMS/SPSC), Graz, Austria, 2022, pp. 1-8, doi: 10.1109/ASMS/SPSC55670.2022.9914723.

[8]. B. Ahmad, D. G. Riviello, A. Guidotti and A. Vanelli-Coralli, “Graph-Based User Scheduling Algorithms for LEO-MIMO Non-Terrestrial Networks.” 2023 Joint European Conference on Networks and Communications & 6G Summit (EuCNC/6G Summit), Gothenburg, Sweden, 2023, pp. 270-275, doi: 10.1109/EuCNC/6GSummit58263.2023.10188287.

[9]. B. Ahmad, D. G. Riviello, A. Guidotti and A. Vanelli-Coralli, “Improved Graph-Based User Scheduling for Sum-Rate Maximization in LEO-NTN Systems.” 2023 IEEE International Conference on Acoustics, Speech, and Signal Processing Workshops (ICASSPW), Rhodes Island, Greece, 2023, pp. 1-5, doi: 10.1109/ICASSPW59220.2023.10193499.

[10]. A. Douik, H. Dahrouj, T. Y. Al-Naffouri and M. -S. Alouini, “A Tutorial on Clique Problems in Communications and Signal Processing.” in Proceedings of the IEEE, vol. 108, no. 4, pp. 583-608, April 2020, doi: 10.1109/JPROC.2020.2977595.

[11]. A. Guidotti and A. Vanelli-Coralli, “Geographical Scheduling for Multicast Precoding in Multi-Beam Satellite Systems.” 2018 9th Advanced Satellite Multimedia Systems Conference and the 15th Signal Processing for Space Communications Workshop (ASMS/SPSC), Berlin, Germany, 2018, pp. 1-8, doi: 10.1109/ASMS-SPSC.2018.8510728.

[12]. ITU-R Radiocommunication Sector of ITU, “Modelling and simulation of IMT networks and systems for use in sharing and compatibility studies (M.2101-0)”, Feb. 2017.

[13]. 3GPP TR 38.811 V15.4.0, “Study on New Radio (NR) to support non-terrestrial networks (Release 15)”, Sep. 2020.

[14]. 3GPP TR 38.821 V16.1.0, “Solutions for NR to support non-terrestrial networks (NTN) (Release 16)”, May 2021.